Process Parameters Optimization in Gas Blow Forming of Pin-type Metal Bipolar Plates using Taguchi and Finite Element Methods

M. Moradian & A. Doniavi*
Department of Mechanical Engineering,
University of Urmia, Iran
E-mail: m.moradian@urmia.ac.ir, a.doniavi@urmia.ac.ir
*Corresponding author

V. Modanloo
Young Researchers and Elite Club, Urmia Branch,
Islamic Azad University, Urmia, Iran
E-mail: v.modanloo@urmia.ac.ir,

V. Alimirzaloo
Department of Mechanical Engineering,
University of Urmia, Iran
E-mail: v.alimirzaloo@urmia.ac.ir

Received: 8 February 2017, Revised: 17 March 2017, Accepted: 18 April 2017

Abstract: Metal bipolar plates are the most important parts of the fuel cells and recently these plates are used instead of graphite ones. In the present study, gas blow forming of a pin-type aluminum 5083 bipolar plate has been studied. After the simulation of the process, the FE model has been validated using experimental results. Then, the effects of parameters including maximum pressure of the gas, pressurization profile and corner radius of the pin on thinning ratio and forming depth of final part have been investigated. Nine experiments were designed using the Taguchi L9 orthogonal array and the experiments were performed using the FE model. The signal to noise (S/N) ratio and the analysis of variance (ANOVA) techniques were carried out to determine the effective parameters and the contribution of each parameter. The maximum pressure of 1.2 MPa, SP2 pressurization profile and corner radius of 0.2 mm lead to the minimum thinning ratio. Also, it was found that to maximize the forming depth, the maximum pressure of 2 MPa, SP1 pressurization profile and corner radius of 0.3 mm should be selected. Also, ANOVA analysis showed that the most significant parameters on thinning ratio and forming depth are corner radius and maximum pressure, respectively.

Keywords: Bipolar plate, Finite element simulation, Gas blow forming, Process parameters

Reference: Moradian, M., Doniavi, A., Modanloo, V., and Alimirzaloo, V., "The Optimization of Process Parameters in Gas Blow Forming of Pin-type Metal Bipolar Plates using Taguchi and Finite Element Methods", Int J of Advanced Design and Manufacturing Technology, Vol. 10/ No. 2, 2017, pp. 101–108.

Biographical notes: M. Moradian is currently a PhD student at Urmia University. His main research interest is metal forming processes. **A. Doniavi** received his PhD from Bath University in UK. His main research interests are design and optimization of processes. **V. Modanloo** is a PhD student. His main research interest is metal forming processes. **V. Alimirzaloo** received his PhD from Amirkabir University of Technology in Tehran.

1 INTRODUCTION

Fuel cells are electrochemical generators used to produce electrical power. Bipolar plates are one of the key components of these cells, thus bipolar plates should be designed as thin as possible [1]. 60-80 percent of weight, 50 percent of volume and 35-45 percent of the cost of a fuel cell is related to bipolar plates [2]. There are four different types of flow patterns used in bipolar plates which are shown in Fig. 1 [3]. Metal bipolar plates are proper alternatives for graphite plates. Good electrical and thermal conductivity and corrosion resistance even in low thickness, are the key properties of these plates [4].

One of the main subjects of recent studies is forming process of metal bipolar plates and many new methods such as hydroforming, rubber pad forming [5] and gas blow forming have been proposed by researchers to form these components. Owsia et al., [6] investigated the forming of stainless steel pin-type plates by hydroforming process. They found that by decreasing the depth-to-width ratio of the die, the thinning ratio decreases and the filling percent increases. Mohammadtabar et al., [7] studied the forming of stainless steel serpentine plates using hydroforming process. Their results showed that increasing the gas pressure not only increases the filling percent but also has a good effect on the thinning behavior of the plate. Gas blow forming is one of the new methods used to form the bipolar plates. The effect of geometrical parameters of die on gas blow forming of conical cups was investigated by Shamsi-Sarband et al., [8]. They stated that by optimizing the geometrical parameters of preform die in a two-stage process, the creep strain will decrease compared to one-stage process. The schematic of gas blow forming process used by Shamsi-Sarband et al. is shown in Fig. 2.

Sun et al., [9] studied the effect of pressurization profile on the deformation characteristics of the sheet during gas blow forming. They found that by use of stepwise pressurization profile, higher dome height with lower strain rate can be achieved. Esmaili et al., [10] investigated the forming of a pin-type aluminum bipolar plate by gas blow forming process. The results of their work showed that increasing the corner radius leads to an increase in the section thickness and increasing gas pressure makes the filling process of part easier. To have a proper comprehension of the gas blow forming of bipolar plates, it is better to optimize input parameters of the process using design of experiments (DOE) method. In this study, the effect of corner radius, maximum pressure and pressurization profile on thinning ratio and forming depth of aluminum 5083 sheet in gas blow forming process is investigated and optimized.

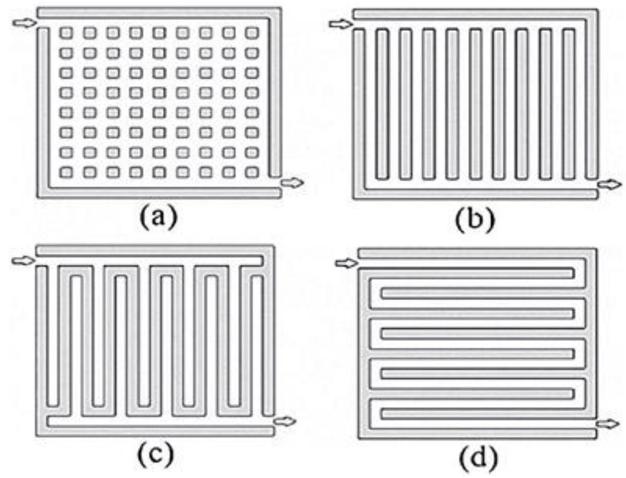

Fig. 1 Illustration of the main flow patterns: (a) Pin-type, (b) Parallel channels, (c) Serpentine, (d) Interdigitated [3]

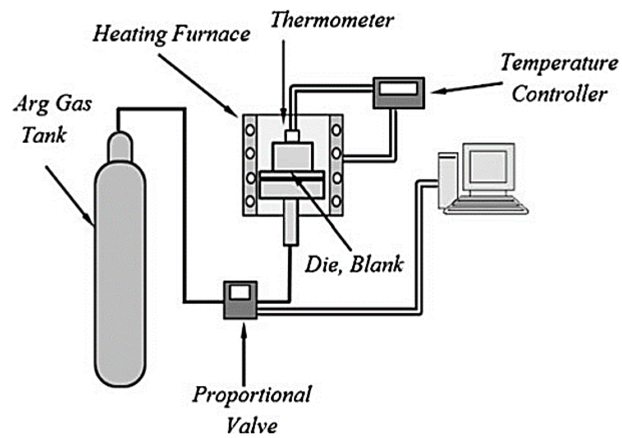

Fig. 2 Schematic of gas blow forming process [8]

2 NUMERICAL SIMULATION

For simulating the gas blow forming process, the commercial ABAQUS software was used [11,12]. Due to symmetry, a quarter of the model was created. The sheet was modeled as a 3D deformable via eight node solid elements (CAX4R). Also, the die was modeled as a rigid body and was meshed with rigid four node shell element (R3D4). The mechanical properties of the 5083 aluminum sheet are given in Table 1. Figure 3 shows the geometrical dimensions of the die in which R is the radius of the edge fillet of the pin (corner radius), S is the diameter of the pin and W is the width of the channel between two adjacent pins also called the cooling channel of a bipolar plate, and the values of R, S, and W are 0.1 mm, 3 mm and 2 mm, respectively. Moreover, the height of the pin is 1 mm.

Table 1 Mechanical properties of aluminum 5083 [10]

Parameter	Value
Yield Stress (MPa)	228
Young's Modulus (GPa)	70.4
Density (kg/m^3)	2260
Poisson's Ratio	0.33

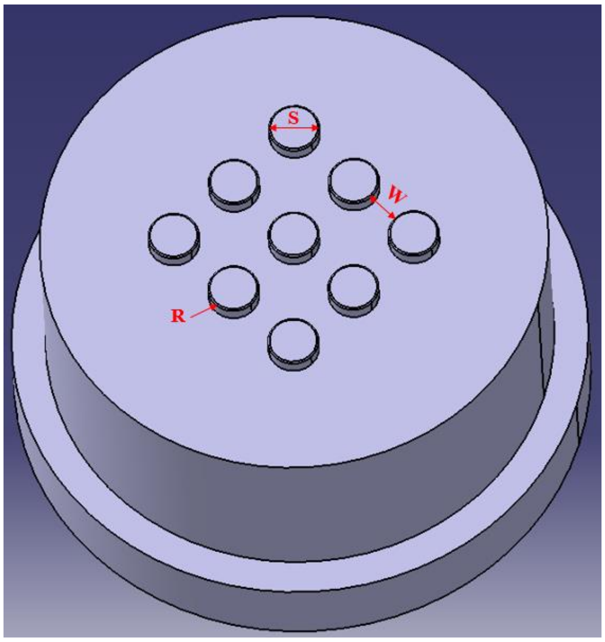

Fig. 3 Schematic geometrical parameters of the die

Penalty contact interface was used in the numerical simulation. A friction coefficient of 0.4 was considered between the sheet and die. The gap between the die and the sheet was fixed at 0.05 mm before the start of the simulation. A gas pressure equal to 1.6 MPa was applied onto the sheet surface.

Figure 4 illustrates the measuring path for the thickness and forming depth in simulation and experiment. It can be observed that the measuring path starts from the center of the middle pin and ends in the center of the side pin. Also, the values of the depth of the nodes (U2) along the measuring path are included in the figure.

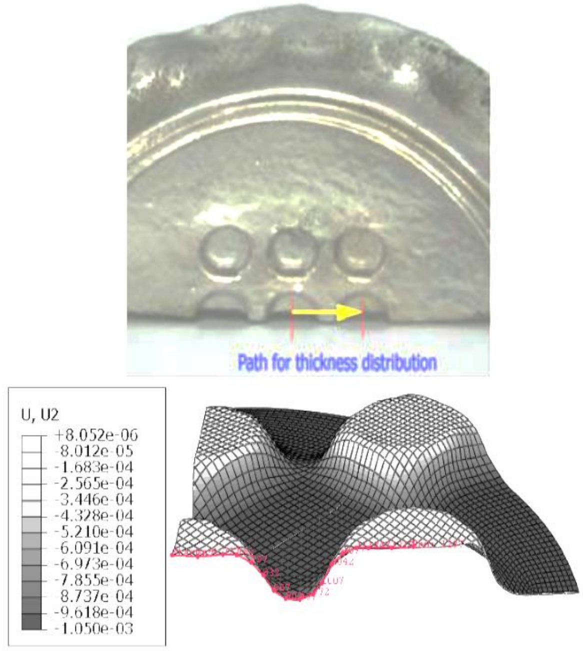

Fig. 4 Measuring path of thickness and depth: (a) Simulation, (b) Experiment [10]

Thickness distribution and filling profile of the formed part are demonstrated in Fig. 5 and Fig. 6, respectively. As it can be seen, there is a good agreement between the simulation results and experimental results of reference [10]. As a result, the validated FE model was further used for parametric study of the gas blow forming process.

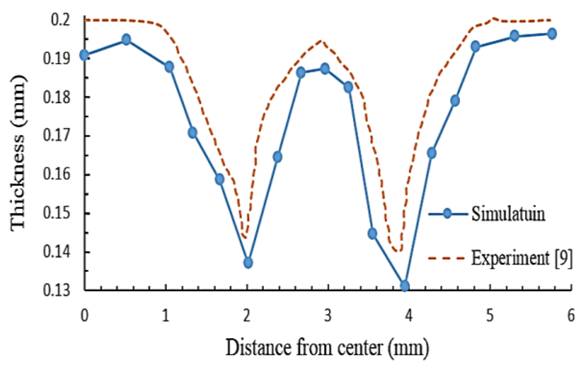

Fig. 5 Thickness distribution of the formed part

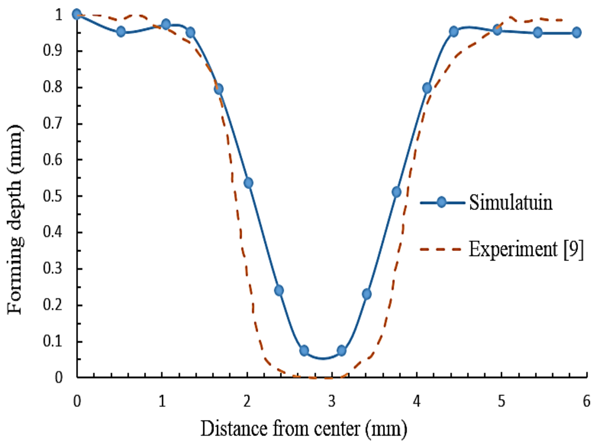

Fig. 6 Filling profile of the formed part

3 DESIGN OF EXPERIMENTS

To investigate the effect of input parameters of process on thinning ratio and the filling depth of the formed part, three parameters in three levels were selected which are shown in Table 2. Three different pressurization profiles used in the experiments are shown in Fig. 7.

Table 2 Input process parameters and their levels

Parameter	Designation	Level Low (1)	Medium (2)	High (3)
Maximum pressure (MPa)	A	1.2	1.6	2
Pressurization profile	B	CP	SP1	SP2
Corner radius (mm)	C	0.1	0.2	0.3

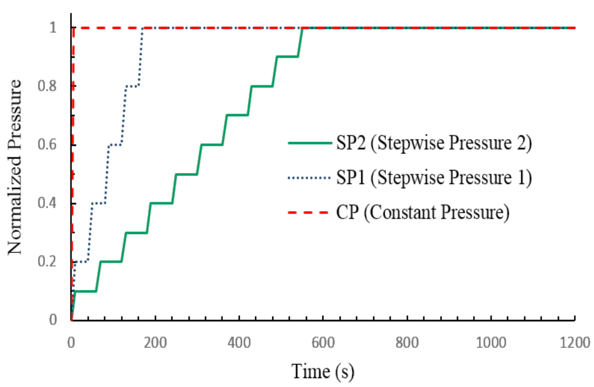

Fig. 7 Different pressurization profiles

Table 3 Taguchi L9 orthogonal array

Trial No.	Maximum pressure (MPa)	Pressurization profile	Corner radius (mm)
1	1.2	CP	0.1
2	1.2	SP1	0.2
3	1.2	SP2	0.3
4	1.6	CP	0.2
5	1.6	SP1	0.3
6	1.6	SP2	0.1
7	2	CP	0.3
8	2	SP1	0.1
9	2	SP2	0.2

Nine experiments were designed using the Taguchi L9 orthogonal array. The experiments are listed in Table 3. Signal to noise (S/N) ratio is defined in the Taguchi approach to determine optimal levels of each parameter. Two equations were used in this study. To minimize the thinning ratio of the sheet, “Smaller is better” state is considered that can be calculated by Equation (1). To maximize the filling depth of the part, “Larger is better” state is that can be calculated by Equation (2).

$$\frac{S}{N} = -10\log\left(\frac{1}{n}\sum_{i=1}^{n} y_i^2\right) \quad (1)$$

$$\frac{S}{N} = -10\log\left(\frac{1}{n}\sum_{i=1}^{n} \frac{1}{y_i^2}\right) \quad (2)$$

4 RESULTS AND DISCUSSION

To evaluate the thinning ratio of the sheet, Eq. (3) was used in which T_0 denotes the initial thickness of the sheet and T_f denotes the minimum thickness of the formed part along the measuring path [13].

$$\%\text{Thinning ratio} = \frac{T_0 - T_f}{T_0} \times 100 \quad (3)$$

Also to determine the filling depth of the formed part, the maximum displacement of the sheet (U2, see Fig. 4) along the measuring path was considered.

4.1. S/N Analysis of Thinning Ratio

After performing the experiments, the thinning ratio of each experiment was obtained which are given in Table 4.

Table 4 The results of thinning ratio

Experiment No.	Thinning ratio (%)
1	57.190
2	49.950
3	50.195
4	52.970
5	52.760
6	57.005
7	55.560
8	59.045
9	52.985

The S/N ratio of each level of input parameters was obtained by importing the results in Minitab software [14] and performing the S/N analysis. As it can be seen in Table 5, S/N analysis gives a rank of importance for parameters that corner radius is the most significant parameter that affects the thinning ratio. Maximum pressure and pressurization profile are ranked second and third important parameters, respectively. The optimal combination of parameters to minimize the thinning ratio was obtained as A1B3C2.

Table 5 S/N ratio results of thinning ratio

Level	Maximum pressure (MPa)	Pressurization profile	Corner radius (mm)
1	-34.38	-34.84	-35.23
2	-34.68	-34.61	-34.31
3	-34.93	-34.54	-34.45
Delta	0.56	0.30	0.92
Rank	2	3	1

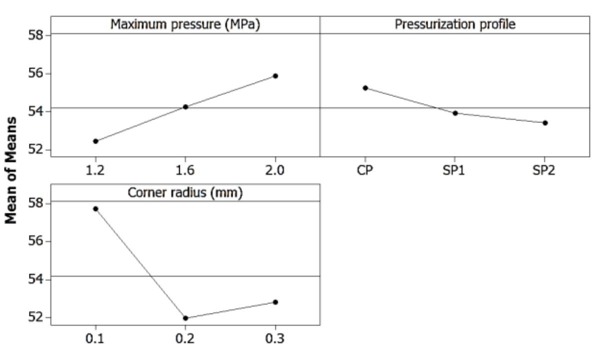

Fig. 8 Main effects plot for means of thinning ratio

Main effects diagram using Minitab software is shown in Fig. 8. It can be seen that by increasing the gas pressure the thinning ratio will increase and to minimize the thinning ratio, the corner radius of pins should be set to 0.2 mm. Among three different pressurization profiles, the Stepwise2 profile is the best option to have less thinning in the sheet.

4.2. ANOVA Analysis of Thinning Ratio

Figure 9 shows the normal probability plot for the thinning ratio. As it is depicted, because of the P-value greater than 0.05 (0.498), the distribution of data is normal [15].

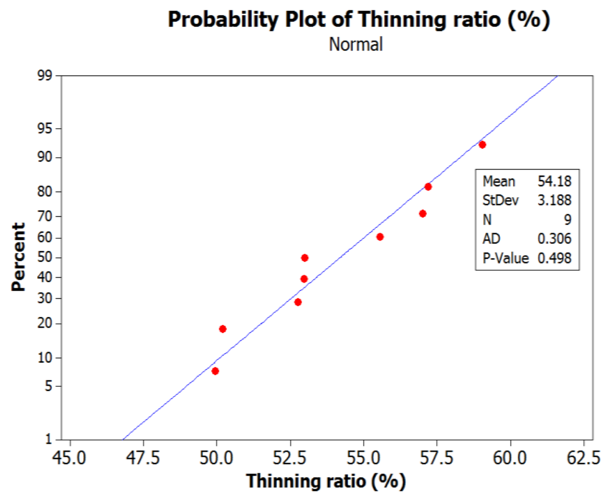

Fig. 9 Normal probability plot for thinning ratio

ANOVA results of thinning ratio are given in Table 6. ANOVA results state that corner radius with the contribution of 71.64% is the most effective parameter. Also, the goodness of the ANOVA model (R-square) was obtained 99.89% that is desirable. All three parameters have an influence on thinning ratio due to p-value less than 0.05.

Table 6 ANOVA result of thinning ratio

Source	Mean Square	P-value	Contribution (%)
Maximum pressure (MPa)	8.772	0.005	21.58
Pressurization profile	2.712	0.016	6.68
Corner radius (mm)	29.119	0.002	71.64
Error	0.044	-	0.1
Total	40.467	-	100

4.3. Confirmation FE Test of Thinning Ratio

When the optimal levels of design parameters have been determined, the final step is to predict and verify the improvement of the quality characteristic using the optimal levels of the design parameters. The optimal levels of parameters for thinning ratio are determined as A1B3C2 from S/N and ANOVA analysis. Table 7 shows the comparison of the predicted thinning ratio and actual thinning ratio from the confirmation FE test that presents a good correlation.

Table 7 Confirmation FE test for thinning ratio

	Optimal Parameters	
	Prediction	FE Test
Parameter levels	A1B3C2	A1B3C2
Thinning ratio (%)	49.439	49.500

Figure 10 shows the formed part using the optimal levels of parameters.

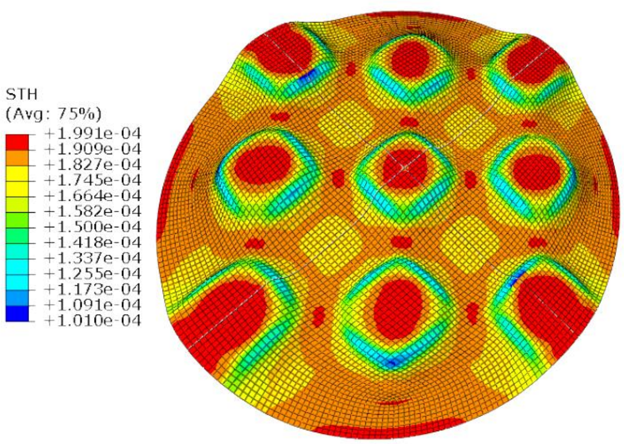

Fig. 10 The formed part using optimal level of parameters (A1B3C2)

4.4. S/N Analysis of Forming Depth

Forming depth results of each experiment are listed in Table 8. The S/N ratio of each level of input parameters was obtained by importing the results in Minitab software and performing the S/N analysis. As it can be seen in Table 9, S/N analysis gives a rank of importance for parameters that the maximum pressure is the most significant parameter that affect the thinning ratio. Corner radius and pressurization profile are ranked second and third important parameters, respectively. The optimal combination of parameters to minimize the forming depth was obtained as A3B2C3.

Table 8 The results of forming depth

Experiment No.	Forming depth (mm)
1	0.761597
2	0.804814
3	0.824971
4	0.943364
5	0.963540
6	0.883510
7	0.998270
8	0.992720
9	0.995380

Table 9 S/N ratio results of forming depth

Level	Maximum pressure (MPa)	Pressurization profile	Corner radius (mm)
1	-1.97427	-0.96232	-1.16824
2	-0.63493	-0.75739	-0.81091
3	-0.03958	-0.92907	-0.66962
Delta	1.93470	0.20493	0.49862
Rank	1	3	2

The main effects diagram is shown in Fig. 11. It can be seen that by increasing the gas pressure, the forming depth of the part will increase. To maximize the forming depth of the part, the corner radius of pins should be maximized. Among three different pressurization profiles, the Stepwise1 profile is the best option to have the most forming depth.

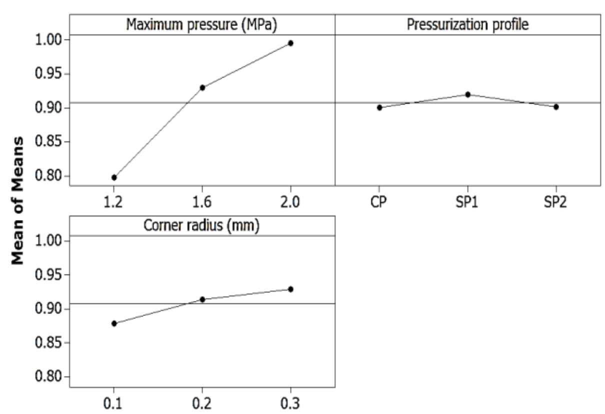

Fig. 11 Main effects plot for means of forming depth

4.5. ANOVA Analysis of Forming Depth

Figure 12 shows the normal probability plot for the forming depth. As it is depicted, because of the P-value greater than 0.05 (0.173), the distribution of data is normal.

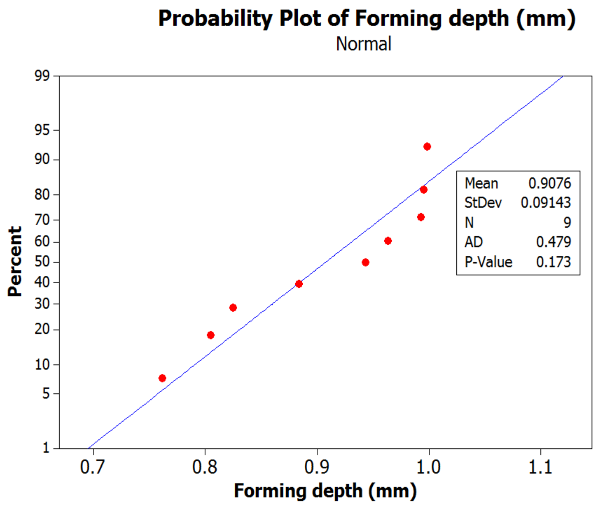

Fig. 12 Normal probability plot for forming depth

ANOVA results of forming depth are given in Table 10. ANOVA results state that maximum pressure with contribution of 91.66% is the most effective parameter. On the other hand, corner radius with contribution of 5.85% and pressurization profile with contribution of 1.11% are almost ineffective parameters on forming depth. Also, the goodness of the ANOVA model (R-square) was obtained 98.61% that is desirable.

Table 10 ANOVA result of forming depth

Source	Mean Square	P-value	Contribution (%)
Maximum pressure (MPa)	0.030646	0.015	91.66
Pressurization profile	0.000368	0.557	1.11
Corner radius (mm)	0.001957	0.191	5.85
Error	0.000463	-	1.38
Total	0.033434	-	100

5 CONCLUSION

In this paper, optimization of process parameters in gas blow forming was investigated using finite element and design of experiments methods. Signal to noise and analysis of variance techniques were used to determine the effect of maximum gas pressure, corner radius and pressurization profile on thinning ratio and forming depth. The results showed that the corner radius is the most effective parameter on thinning ratio. Also, it was obtained that the maximum pressure is the most effective parameter on forming depth. The stepwise pressurization profiles have positive effect on thinning ratio and forming depth. The results of this paper can be useful for researchers that study gas blow forming process.

6 REFERENCES

[1] Middelman, E., Kout, W., Vogelaar, V., Lenssen, J., and Waal, E.; “Bipolar Plates for PEM Fuel Cells”, Journal of Power Sources, Vol. 118, No. 1-2, 2003, pp. 44-46.

[2] Mahabunphachai, S.; “A Hybrid Hydroforming and Mechanical Bonding Process for Fuel Cell Bipolar Plates”, PhD. Dissertation, University of Michigan, 2008.

[3] Heinzel, A., Mahlendorf, F., and Jansen, C., Bipolar Plates, Elsevier, Duisburg, 2009.

[4] Wang, H. L., Sweikart, M. A., and Turner, J. A.; “Stainless Steel as Bipolar Plate Material for Polymer Electrolyte Membrane Fuel Cells”, Journal of Power Sources, Vol. 115, No. 2, 2003, pp. 243-251.

[5] Elyasi, M., Khatir, F.A., and Hosseinzadeh, M.; “Manufacturing Metallic Bipolar Plate Fuel Cells Through Rubber Pad Forming Process”, The International Journal of Advanced Manufacturing Technology, 2016, pp. 1-13.

[6] Belali Owsia, M., Hosseinipour, S. J., Bakhshi-Jooybari, M., and Gorji, A.; “The Experimental and Simulation Investigation of Process and Geometrical Parameters for Hydroforming of Pin-type Metallic Bipolar Plates”, Modares Mechanical Engineering, Vol. 15, No. 7, 2015, pp. 215-226.

[7] Mohammadtabar, N., Bakhshi-Jooybari, M., and Hosseinipour, S.J.; “Study of Effective Parameters in Hydroforming of Fuel Cell Metallic Bipolar Plates with Parallel Serpentine Flow Field”, Modares Mechanical Engineering, Vol. 14, No. 8, 2014, pp. 17-27.

[8] Shamsi-Sarband, A., Hosseinipour, S. J., Bakhshi-Jooybari, M., and Shakeri, M.; “The Effect of Geometric Parameters of Conical Cups on the Preform Shape in Two-Stage Superplastic Forming Process”, Journal of Materials Engineering and Performance, Vol. 22, No. 12, 2013, pp. 3601-3611.

[9] Sun, P., Wu, H., Tsai, H., Huang, C., and Tzou, M.; “Effect of Pressurization Profile on the Deformation Characteristics of Fine-grained AZ31B Mg Alloy Sheet During Gas Blow Forming”, Journal of Materials Processing Technology, Vol. 210, 2010, pp. 1673-1679.

[10] Esmaeili, S., Hosseinipour, S. J., Shamsi-Sarband, S.; “Simulation and Experimental of Metallic Bipolar Plates for Fuel Cell by Gas Blow Forming Process”, National conference on Mechanical Engineering, Malayer, Iran, 2013.

[11] Kadkhodayan, M., Pourhasan, P.; "Finite Element Simulation of Process and Springback of Friction Aided Deep Drawing Using Tapered Blank Holder Divided Into Eight Segments", International Journal advanced Design and Manufacturing Technology, Vol. 3, No. 4, 2010, pp. 1-10.

[12] Alimirzaloo, V., Modanloo, V; "Minimization of the Sheet Thinning in Hydraulic Deep Drawing Process Using Response Surface Methodology and Finite Element Method", International Journal of Engineering (IJE), Transactions B: Applications, Vol. 29, No.2, 2016, pp. 264-273.

[13] Modanloo, V., Gorji, A., and Bakhshi-Jooybari, M.; "Effects of Forming Media on Hydrodynamic Deep Drawing", Journal of Mechanical Science and Technology, Vol. 30, No. 5, 2016, pp. 2237-2242.

[14] Kolahdoozan, M., Azimifar, F., and Yazdi, S. R.; "Finite Element Investigation and Optimization of Tool Wear in Drilling Process of Difficultto-Cut Nickel-Based Superalloy using Response Surface Methodology", International Journal Advanced Design and Manufacturing Technology, Vol. 7, No. 2, 2014, pp. 67-75.

[15] Modanloo, V., Hasanzadeh, R. and Esmaili, P.; "The Study of Deep Drawing of Brass-steel Laminated Sheet Composite Using Taguchi Method", International Journal of Engineering (IJE), Transactions A: Basics, Vol. 29, No.1, 2016, pp. 103-108.